Progress in Organic Coatings 71 (2011) 343–349

Contents lists available at ScienceDirect

Progress in Organic Coatings

journal homepage: www.elsevier.com/locate/porgcoat

Corrosion inhibition of mild steel by natural product compound

M.A. Ameer*, A.M. Fekry

Chemistry Department, Faculty of Science, Cairo University, Giza 12613, Egypt

ARTICLE INFO

Article history:
Received 4 December 2010
Received in revised form 6 March 2011
Accepted 1 April 2011

Keywords:
Inhibition
EIS
SEM
Mild steel
IPMP

ABSTRACT

Corrosion inhibition of mild steel in H_3PO_4 containing chloride or sulphate ions have been studied using different electrochemical techniques. The corrosion and hydrogen evolution of mild steel alloy in 2 M H_3PO_4 acid containing 0.5 M NaCl can be effectively inhibited by addition of natural product compound, Thymol (IPMP), of different concentrations. However, in 2 M H_3PO_4 containing 0.5 M Na_2SO_4 corrosion cannot be effectively inhibited. The results of electrochemical impedance spectroscopy (EIS) and potentiodynamic polarization measurements confirm the synergistic effects which describe the increase in the effectiveness of a corrosion inhibitor in the presence of Cl^- ions in the corrosive medium. At any temperature, an increase in it leads to an increase of the corrosion rate and hydrogen evolution on mild steel. Polarization and EIS results are in good agreement with each other. The obtained results were confirmed by surface examination using scanning electron microscope.

1. Introduction

The use of inhibitors for the control of corrosion for metals and alloys which are in contact with aggressive environment is an accepted practice. Large numbers of organic compounds were studied to investigate their corrosion inhibition potential. All these studies reveal that organic compounds especially those with N, S and O showed significant inhibition efficiency. But, unfortunately most of these compounds are not only expensive but also toxic to living beings [1]. It is needless to point out the importance of cheap, safe inhibitors of corrosion. Plant extracts have become important as an environmentally acceptable, readily available and renewable source for wide range of inhibitors. They are the rich sources of ingredients which have very high inhibition efficiency. Acid solutions are widely used in many industrial processes [2]. Besides hydrochloric acid, phosphoric acid and sulphuric acid are regular aggressive solutions for acid cleaning and acid descaling due to their special chemical properties. The use of corrosion inhibitor is one of the most practical methods for protecting the corrosion of metal and decreasing hydrogen evolution. As a result, corrosion inhibitors for hydrochloric acid, phosphoric acid and sulphuric acid have attracted increasing attention due to their extended applications [1–5]. The protection of metals against corrosion by H_3PO_4 has been the subject of much study since it has been used in many industrial processes especially in fertilizer production [6–11]. It is well known that halide ions improve the inhibition efficiency of organic molecules through synergism, but the data on the synergism between organic corrosion inhibitor and halide ions on metal corrosion in H_3PO_4 solution are meager. Corrosion inhibitors can be used to prevent metal from corrosion in corrosive media and decrease hydrogen evolution. Generally the studies on corrosion inhibitors are mainly focusing on three domains: one is to find appropriate inhibitor among the known compounds, and the next is to synthesize new compounds under the direction of theoretical calculation, and the last is searching the synergistic action among various compounds to expand the range of inhibitor applications. Many works have studied the influence of organic compounds containing nitrogen, sulphur, oxygen, and phosphorus on the corrosion of steel in acidic media. The results show that most organic compounds employed as corrosion inhibitors can adsorb on the metal surface through heteroatoms such as nitrogen [10], sulphur [12–15], oxygen [13], phosphorus [16] and multiple bonds etc. preventing steel from corrosion. Different concentrations of Thymol were investigated as corrosion inhibitors for mild steel in 2 M H_3PO_4 solution at different temperatures using AC impedance spectroscopy and polarization techniques. AC impedance results were interpreted using an equivalent circuit in which a constant phase element (CPE) was used in place of a double layer capacitance (C_{dl}) in order to give more accurate fit to the experimental results. The experimental results showed that the compound inhibits the corrosion to some extent. The study was carried out in the absence and presence of chloride or sulphate ions. The inhibition efficiency increased with concentration in the presence of Cl^- ions. The scheme of Thymol (IPMP) is as follows:

* Corresponding author. Tel.: +20 10 1675085.
E-mail address: mameer_eg@yahoo.com (M.A. Ameer).

0300-9440/$ – see front matter © 2011 Elsevier B.V. All rights reserved.
doi:10.1016/j.porgcoat.2011.04.001

Table 1
The chemical compositions of mild steel (wt%).

C	Si	Mn	P	S	Cu	Cr	Mo	Ni	Sn	V
0.31	0.21	0.81	0.014	0.017	0.06	0.02	0.01	0.02	0.0	0.002

The balance is the wt% of Fe in the steel.

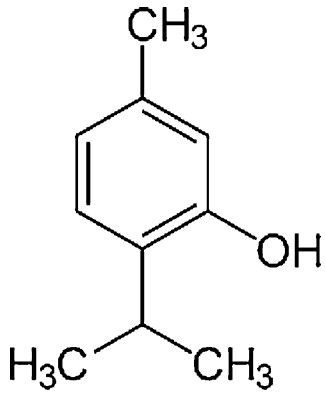

IPMP

IPMP is 2-isopropyl-5-methylphenol, (IPMP) (molar mass = 150.22 g mol^{-1}) which is a natural monoterpene phenol derivative of cymene, $C_{10}H_{14}O$, isomeric with carvacrol, found in oil of thyme, and extracted as a white crystalline substance of a pleasant aromatic odor and strong antiseptic properties.

The main aim of this research work is to study the electrochemical behavior of mild steel in different concentrations of naturally aerated NaCl or Na_2SO_4 in 2 M H_3PO_4 solutions at different temperatures using electrochemical techniques and surface examination. Also, the effect of adding IPMP as corrosion inhibitor for mild steel is studied.

2. Material and methods

The steel rod was tested in the present study with its cross-sectional area of 0.47 cm^2. The chemical composition of the steel, as given by the supplier, is listed in Table 1. The test aqueous solutions contained H_3PO_4, NaCl (Aldrich), Na_2SO_4 (BDH) and IPMP with different concentrations. Triple distilled water was used for preparing all solutions. In all measurements, mechanically polished electrode was used. Polishing was affected using successively finer grade of emery papers (600–1200 grade). Polarization and electrochemical impedance spectroscopy (EIS) measurements were carried out using the electrochemical workstation IM6e Zahner-electrik GmbH, Meβtechnik, Kronach, Germany. The excitation AC signal had amplitude of 10 mV peak to peak in a frequency domain from 0.1 Hz to 100 kHz. The EIS was recorded after reading a steady state open-circuit potential. The scanning was carried out at a rate of 30 mV min^{-1} over the potential range from −1000 to 0 mV vs. saturated calomel electrode (SCE). Prior to the potential sweep, the electrode was left under open-circuit in the respective solution for ~1 h until a steady free corrosion potential was recorded. Corrosion current density, i_{corr}, which is equivalent to the corrosion rate, is given by the intersection of the Tafel lines extrapolation. Because of the presence of a degree of nonlinearity in the Tafel slope part of the obtained polarization curves, the Tafel constants were calculated as a slope of the points after E_{corr} by ±50 mV using a computer least-squares analysis. i_{corr} were determined by the intersection of the cathodic Tafel line with the open-circuit potential. To study the effect of temperature, the cell was immersed in water thermostat in the temperature range of 298–328 K. For surface examination, the electron microscope used is JEOL-JEM-100s type with magnification of 100×.

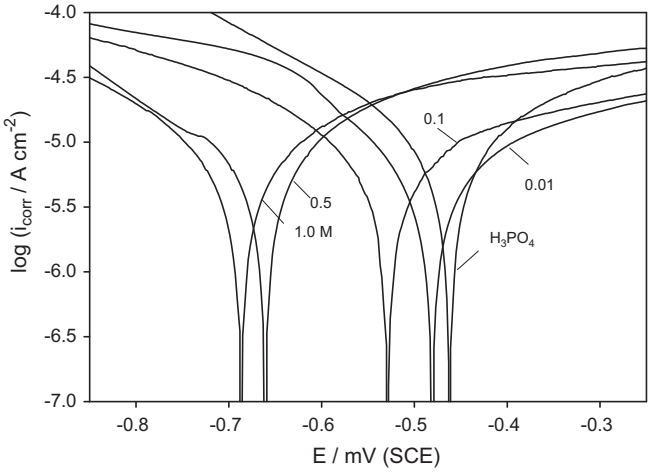

Fig. 1. Potentiodynamic polarization curves of steel in 2 M H_3PO_4 with different concentrations of SO_4^{2-}.

Table 2
Equivalent circuit and corrosion parameters of mild steel after 1 h immersion for different concentrations of Na_2SO_4, NaCl or 0.5 M NaCl containing different concentrations of IPMP, in 2.0 M H_3PO_4 at 298 K.

[conc.] (M)	R_0 (Ω cm^2)	R_1 (kΩ cm^2)	Q_1 (Ω^{-1} s$^\alpha$ cm^{-2})	α_1	R_2 (kΩ cm^2)	Q_2 (Ω^{-1} s$^\alpha$ cm^{-2})	α_2	i_{corr} (μA cm^{-2})	E_{corr} (V)
[H_3PO_4]									
2.0	6.6	3.11	6.5	0.93	0.341	17.2	0.99	0.23	−0.46
[NaCl]									
0.01	3.6	16.83	35.0	0.83	0.164	278.8	0.99	0.35	−0.65
0.10	3.0	3.84	100.4	0.83	0.097	342.5	0.84	2.06	−0.72
0.50	3.1	3.29	480.8	0.89	0.090	952.2	0.83	2.75	−0.81
1.00	2.6	20.63	36.5	0.91	0.276	38.2	0.81	0.27	−0.49
[Na_2SO_4]									
0.01	11.2	16.11	18.0	0.81	0.170	152.2	0.96	0.28	−0.48
0.10	1.8	15.23	27.3	0.86	0.123	321.1	0.99	0.41	−0.53
0.50	1.2	9.09	33.5	0.84	0.098	322.4	0.99	0.56	−0.66
1.00	1.2	5.75	34.1	0.84	0.063	370.1	0.96	0.90	−0.69
[IPMP] (mM) in presence of 2 M H_3PO_4 + 0.5 M Cl^-									
0.1	15.3	9.49	115.1	0.89	2.045	515.1	0.97	1.09	−0.78
0.1	8.6	9.30	117.1	0.89	0.723	541.3	0.96	0.852	−0.76
5.0	5.5	21.50	119.6	0.89	5.114	552.4	0.98	0.475	−0.74
10.0	3.3	29.80	214.2	0.95	8.608	570.1	0.99	0.264	−0.69

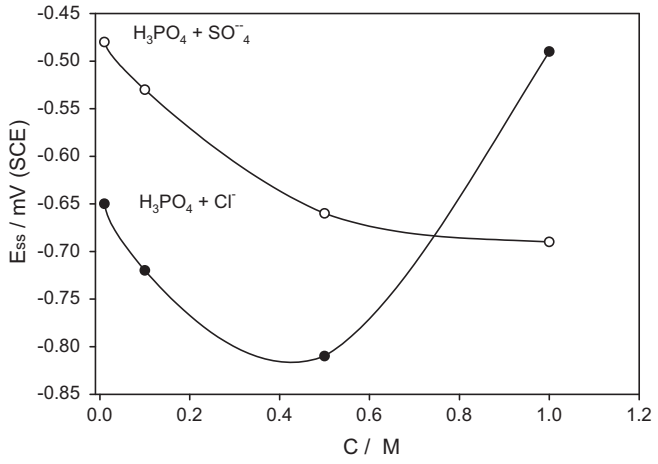

Fig. 2. Variation of E_{SS} of the steel with the concentration of Cl^- or SO_4^{2-} in 2 M H_3PO_4.

3. Results and discussion

3.1. Potentiodynamic polarization measurements

In this part the potentiodynamic polarization behavior of steel was studied in relation to anion nature and concentration of the aqueous solutions. Fig. 1 shows a typical linear sweep potentiodynamic trace for the steel in 2 M H_3PO_4 without and with different concentrations of Na_2SO_4 solutions (as an example). The polarization curves were obtained for different concentrations of Na_2SO_4 in 2 M H_3PO_4 solution. It is noticed that the corrosion potential shifts towards more anodic potential as the concentration decreases as shown in Table 2. A difference of 200 mV is measured between the corrosion potential of the steel in 0.01 and 1.0 M Na_2SO_4. In the anodic range a current plateau is observed. Fig. 2 represents the relation of the steady state potential (E_{SS}) and the concentration of NaCl or Na_2SO_4 in 2 M H_3PO_4 solutions. It is noticed that the corrosion potential shifts considerably to active direction indicating that these salts depolarize the anodic reaction, i.e., promote the dissolution of iron from the steel. For the tested steel the estimated i_{corr} is illustrated in Fig. 3 as a function of the concentration of NaCl or Na_2SO_4 in 2 M H_3PO_4. The results indicate clearly that (i_{corr}) is dependent on the anion type and concentration of the medium. Fig. 3 shows the relation of corrosion current density and the molar concentration of NaCl or Na_2SO_4 in 2 M H_3PO_4 at 298 K. Generally, the results are drawn as follows: at a fixed anion concentration, the value of i_{corr} is always higher in chloride anion compared to

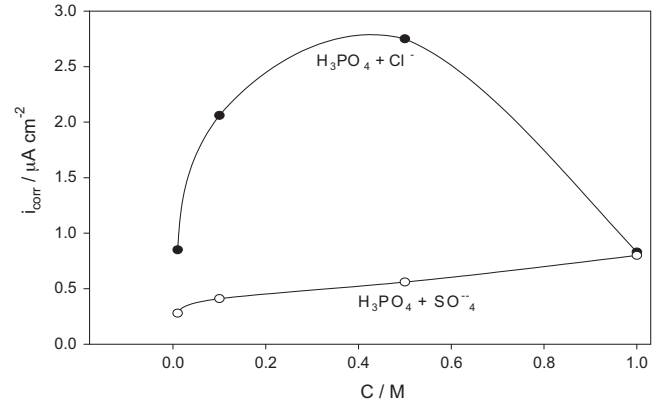

Fig. 3. Variation of i_{corr} of the steel with the concentration of Cl^- or SO_4^{2-} in 2 M H_3PO_4.

Table 3
Inhibition efficiencies of mild steel alloy at different concentrations of IPMP at 298 K.

$C_{inhibitor}$ (mM)	IE% Tafel	IE% EIS
0.1	60.2	70.7
1.0	69.0	66.2
5.0	82.7	87.3
10	90.4	91.2

sulphate anion in 2 M H_3PO_4. In 2 M H_3PO_4 solutions with addition of NaCl, Figs. 2 and 3, the values of both E_{SS} and i_{corr} increase with increasing the concentration (<0.5 M). At concentration ≥ 0.5 M, the values have a shift drop. As far as the present results are concerned, it is possible to assume that Cl^- can participate in enhancing the formation of soluble oxochloro complexes which initiate pit nucleation at the active inclusion sites leading to an increase in the corrosion rate or i_{corr} and E_{SS} tends to more negative values. Increasing the Cl^- concentration (>0.5 M) suppresses the solubility of these species. A possible concomitant hydrolysis reaction cannot be also excluded which generates insoluble salts or hydroxides that hinder contact between the metallic surface and the electrolyte solution in the pit with a consequent decrease in the corrosion rate associated with decreasing i_{corr} and E_{SS} value shifts positively. These results are consistent with those reported by Ogura et al. [17]. The corrosion rate and hydrogen evolution was found to be higher in the acid containing chloride ion as compared with the acid containing sulphate ion at a comparable concentration [18,19]. The significant difference in the i_{corr} values between Cl^- and SO_4^{2-} media may possibly be due to the difference in the extent of incorporation of the oxide film on the steel surface by the electrolyte species during the anodization process. Also the effect of IPMP concentration (0.1–10 mM) as inhibitor is studied in 2 M H_3PO_4 solution containing 0.5 M chloride or 0.5 M sulphate solutions. The corrosion parameters are given in Table 2 and the inhibition efficiency (IE%) are calculated, Table 3, from the following equation [13]:

$$IE\% = 1 - \frac{i_{inh}}{i_{corr}} \times 100 \quad (1)$$

where i_{corr} and i_{inh} are the uninhibited and inhibited corrosion current densities, respectively. It can be seen from the experimental results derived from polarization curves that increasing IPMP concentration in presence of 0.5 M Cl^- decreased i_{corr} and hydrogen evolution at all of the studied concentrations. The change of cathodic and anodic Tafel slopes alters unremarkably in the presence of the inhibitor. This is indicative that the inhibitor acts by merely blocking the reaction sites of the metal surface without changing the anodic and cathodic reaction mechanisms [2]. Both the anodic and cathodic current densities were decreased indicating that IPMP suppressed both the anodic and cathodic reactions. Also it was found that the IE increases till 81.5% at 10 mM IPMP concentration in presence of Cl^- as shown in Fig. 4. The order of IE increases as follows: H_3PO_4 + IPMP + Cl^- > H_3PO_4 + IPMP > H_3PO_4 + IPMP + SO_4^{2-}. It is apparent that sulphate ions hinder IPMP adsorption, thus IE is less than that in phosphoric acid only. This may be due to that in presence of sulphate ions the salts formed in the pits are somewhat more soluble than in its absence.

Some studies [20,21] show Thyme, which contains the powerful anticeptic thymol has the active ingredient, offers excellent protection for steel and decrease hydrogen evolution. NaCl has been used to improve the inhibition efficiency of inhibitor; this phenomenon has been frequently used in practice due to its efficiency and low effective cost [22,23].

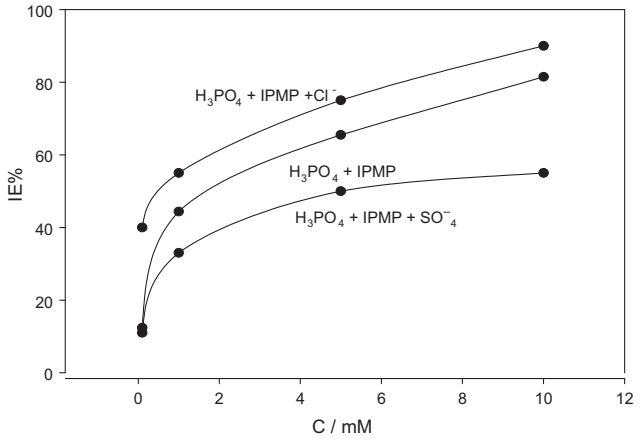

Fig. 4. Variation of IE% with the concentration of IPMP.

3.2. EIS measurements

Fig. 5a and b shows the EIS data for the steel traced at the rest potential in 2 M H_3PO_4 solutions with different concentrations (0.01–1.0 M) of NaCl or Na_2SO_4, respectively. In all cases the impedance Bode data display two maximum phase lags, indicating the presence of two time constants corresponding to different corrosion or passivation steps. It is also clear that at both low frequencies the slopes of log$Z$–log$f$ relations deviate from the value of −1 and the phase angle maxima, θ_{max}, is far away from 90°, which are required in case of pure capacitive behavior [18]. The

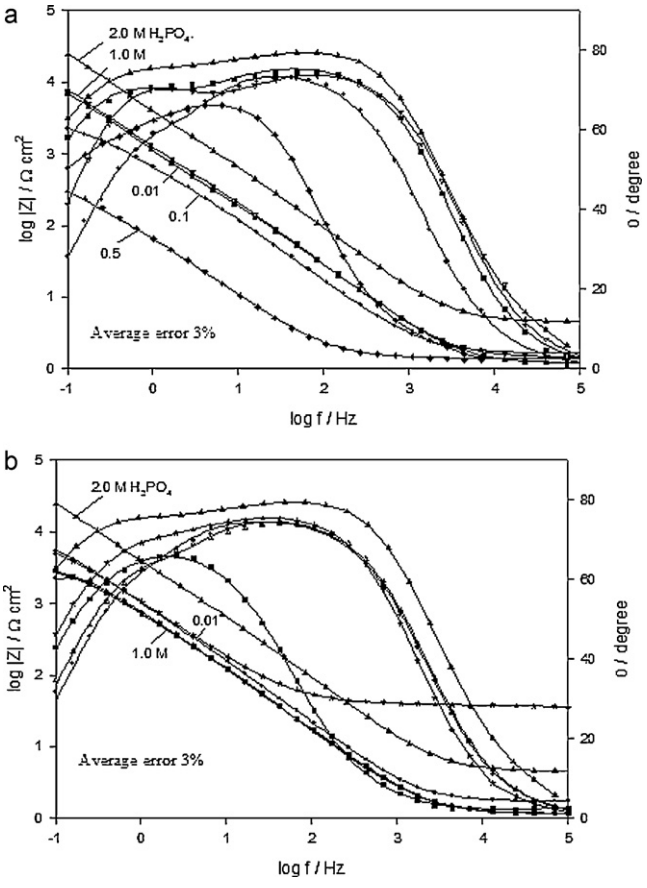

Fig. 5. Bode plots of steel in different concentrations of (a) Cl^- or (b) SO_4^{2-} solution in 2 M H_3PO_4.

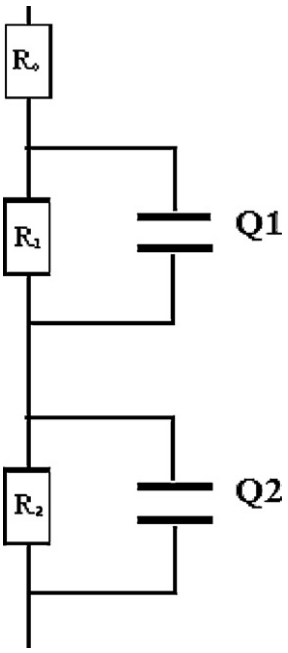

Fig. 6. Equivalent circuit model representing two time constants for an electrode/electrolyte solution interface.

curves move downwards and the impedance decreases. But the overall impedance curve maintains its extremely straight character except at the lowest frequencies the slope of that line becomes significantly less than −1, accompanied by a phase angle less than 90°. The appearance of a shoulder on the phase angle curves at lower frequencies, which shifts the curves into two different frequency regions, is the response of at least two different frequency-dependent processes with corresponding time constants. The five elements RQ equivalent circuit with two lumped time constants is necessary for modeling faradaic processes involving the adsorption of two different species as shown in Fig. 6. This circuit has several structures: one of them is the Voight model, where its impedance expression is as follows [24]:

$$Z(\omega) = R_0 + \frac{R_1}{1 + R_1 Q_1 (j\omega)^{\alpha_1}} + \frac{R_2}{1 + R_2 Q_2 (j\omega)^{\alpha_2}} \quad (2)$$

with $0 \le \alpha_1, \alpha_2 \le 1$.

The passive film can be considered as the dielectric plates capacitor formed between the metallic substrate and the counter electrode. Fitting procedures have shown that good agreement between the theoretical and experimental data is obtained if a frequency-dependent constant phase element (CPE) is introduced instead of pure capacitor, where Q, with the units of $\Omega^{-1}\,s^{\alpha}$, is a general admittance function has a combination of properties related to both the surface and electroactive species and is independent of the frequency (f). The equivalent circuit parameters are tabulated in Table 2. This EEC consists of two circuits in series from R_1Q_1 and R_2Q_2 parallel combination and the two are in series with the solution resistance (R_0). By this way Q_1 is related to combinations from the capacitance of the porous (outer) layer and Q_2 of the barrier inner layer while R_1 is the resistance of the sealed pores by the corrosion products in the outer layer and R_2 of the barrier layer [24,25]. For this model, the relation gives the reciprocal capacitance of the surface film that is directly proportional to its thickness [26]:

$$C^{-1} = Q_1^{-1} + Q_2^{-1} \quad (3)$$

The simulated response of the representative circuit compares well with the experimental results both in admittance and impedance planes. This indicates that the suggested model is suitable for

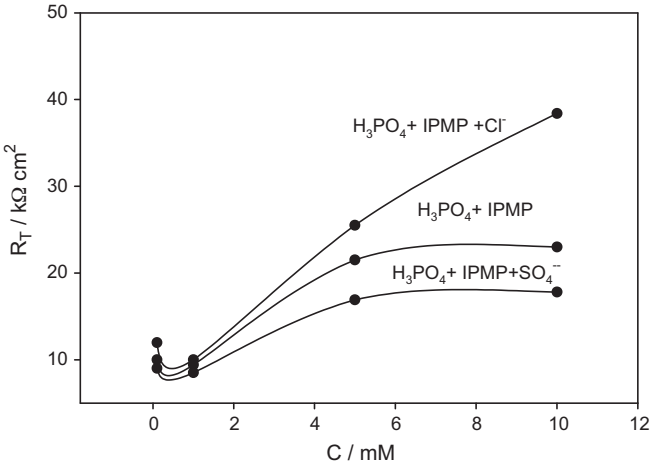

Fig. 7. Variation of R_T values of steel with concentration of IPMP in 2 M H_3PO_4 solutions without and with 0.5 M Cl^- or 0.5 M SO_4^{2-}.

explaining the behavior of the steel in phosphoric acid with chloride or sulphate solutions over the concentration range studied. The equivalent circuit parameters are presented in Table 2. In our study the values of α_1 and α_2 are from 0.81 to 0.99. Fig. 7 represents the variation of R_T ($R_1 + R_2$) values of steel with concentration of IPMP in 2 M H_3PO_4 solutions without and with 0.5 M Cl^- or 0.5 M SO_4^{2-}. The data indicates that R_T values for steel in H_3PO_4 containing Cl^- increase with increasing IPMP concentrations but in case of absence and presence of SO_4^{2-}, the relation shows a limited increase. As far as the present results are concerned, a possible concomitant hydrolysis reaction cannot be also excluded which generates insoluble salts or hydroxides that hinder contact between the metallic surface and the electrolyte solution in the pit with a consequent decrease in the corrosion rate associated with an increase in R_T value [27,28]. The effect of IPMP concentration (0.1–10 mM) as inhibitor is studied in 2 M H_3PO_4 solution containing 0.5 M chloride solution and shown in Fig. 8 as Nyquist plots. The diameter of the depressed uncompleted circles increases with increasing IPMP concentration which suggests that the formed surface film increased in its stability with increasing inhibitor concentration. It is well known that chloride ions have a smaller degree of hydration, and they can bring excess negative charges in the vicinity of the interface due to specific adsorption, then, positively charged ions may adsorb onto the surface. In the present study, IPMP may be protonated in the acid solution. Since steel surface contains positive charges in the acid

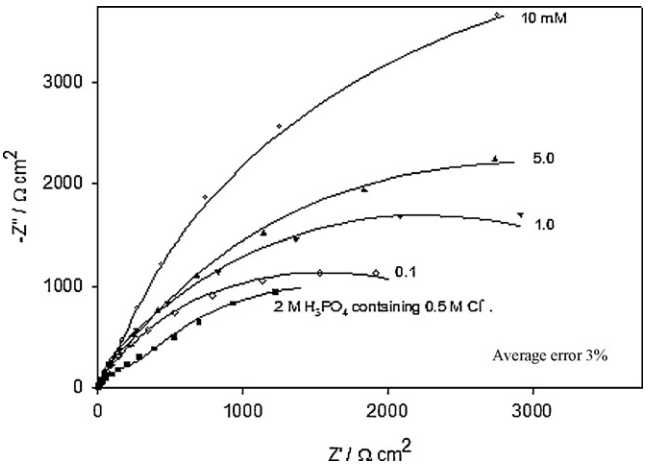

Fig. 8. Nyquist plots of steel in different concentrations of IPMP inhibitor with 2 M H_3PO_4 containing 0.5 M Cl^-.

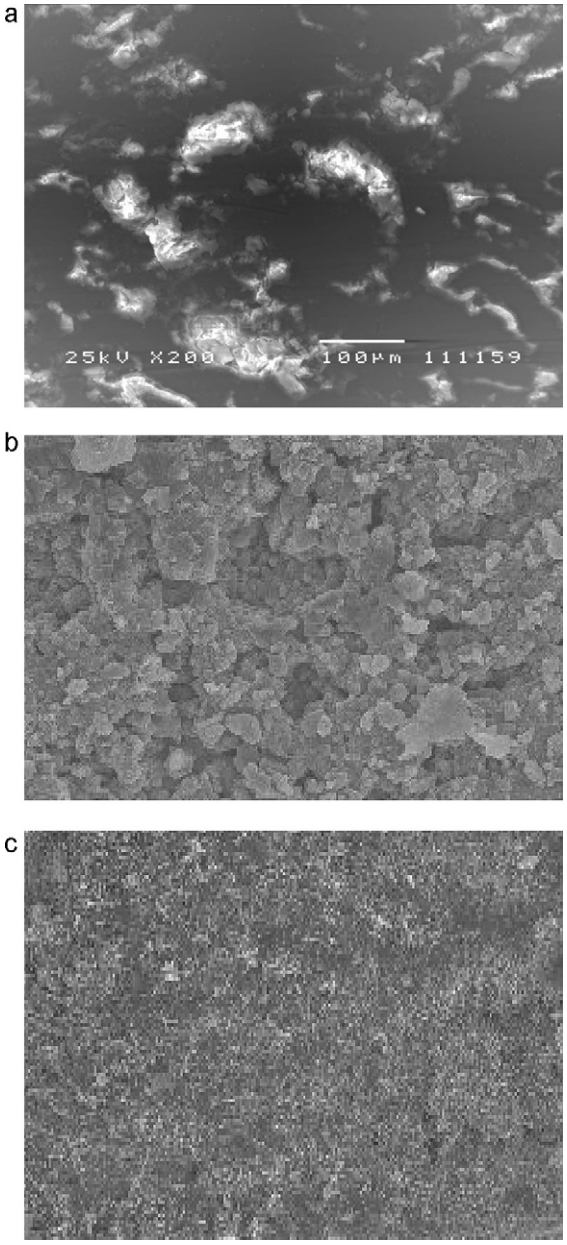

Fig. 9. SEM graphs for the steel in (a) 2 M H_3PO_4 containing 0.5 M Cl^-, (b) 2 M H_3PO_4 containing 0.5 M Cl^- + 0.1 mM IPMP and (c) 2.0 M H_3PO_4 containing 0.5M Cl^- + 10 mM IPMP.

solution, results can be explained on the assumption that in the presence of Cl^-, the negatively charged Cl^- would attach to positively charged surface. Then, near the interface, the concentrations of Cl^- and protonated IPMP are much higher than those in bulk solution, the protonated IPMP do not attach directly to the positively charged steel surface because of repulsive interaction between the protonated IPMP and the positively charged steel surface. The protonated IPMP, however, can attach to the steel surface by means of electrostatic interaction between Cl^- and protonated IPMP. When IPMP adsorbs on metal surface, coordinate bond is formed by partial transference of electrons from the polar atom (O atom) of IPMP to the metal surface [29].

The results were confirmed using surface examination. All corroded specimens were rinsed gently with distilled water, dried and stored in a desiccator for several days before they were examined by scanning electron microscopy (SEM). Fig. 9a–c represents an example for the SEM image for tested electrode in 2 M H_3PO_4 with 0.5 M

NaCl (Fig. 9a), in 0.1 mM IPMP (Fig. 9b) and in 10 mM IPMP (Fig. 9c). Fig. 9a is corroded and contain a lot of pits suggesting that a chloride ion is so aggressive at this concentration. However, for 0.1 mM IPMP in 2 M H_3PO_4 with 0.5 M NaCl the image is smoother than blank. Also, Fig. 9c is for 10 mM IPMP in 2 M H_3PO_4 with 0.5 M NaCl; it shows that the film is much more improved at high concentration forming a film in the form of a net.

3.3. Mechanism of the inhibition of corrosion

The inhibition efficiency of Thymol could be due to the substitution of terminal hydrogen of phenyl ring by alkyl group that contain higher number of carbon atom, in addition to the aromatic phenyl ring donating higher electron density group. It is well known that chloride ions have a smaller degree of hydration, thus they could bring excess negative charges in the vicinity of the interface, and then, positively charged ions might adsorb onto the surface. In the present study, IPMP might be protonated in the acid solution according to the mechanism which involving two adsorbed intermediates has been used to account for the retardation of Fe anodic dissolution in the presence of an inhibitor [30,31]:

$$Fe + H_2O \rightarrow Fe \cdot H_2O_{ads} \quad (4a)$$

$$Fe \cdot H_2O_{ads} + inh \rightarrow Fe\ inh^-_{ads} + H^+ + inh \quad (4b)$$

$$Fe \cdot H_2O_{ads} + inh \rightarrow Fe\ inh_{ads} + H_2O \quad (4c)$$

$$FeOH^-_{ads} \xrightarrow{rds} FeOH_{ads} + e \quad (4d)$$

$$Fe\ inh_{ads} \rightarrow Fe\ inh^+_{ads} + e \quad (4e)$$

$$FeOH_{ads} + Fe\ inh^+_{ads} \rightarrow Fe\ inh_{ads} + FeOH^+ \quad (4f)$$

$$FeOH^+ + H^+ \rightarrow Fe^{2+} + H_2O \quad (4g)$$

where inh represents the inhibitor species.

According to the detailed mechanism above, displacement of some adsorbed water molecules on the metal surface by inhibitor species to yield the adsorbed intermediate Fe inh_{ads} (Eq. (4c)) reduces the amount of the species Fe inh^-_{ads} available for the rate determining step. From the observed results it can be inferred that the insoluble Fe–IPMP complexes dominates the adsorbed intermediates and thus the resultant has inhibitive effects. This conclusion is in line with those of Jaen et al. [32].

With high inhibitor concentrations, a compact and coherent inhibitor overlayer forms on the mild steel surface, reducing chemical attack of the metal. The adsorption of an organic molecule on the surface of the mild steel is regarded as a substitution adsorption process between the organic compound in the aqueous phase (Org_{aq}) and the water molecules adsorbed on the mild steel surface (H_2O_{ads}) [33]:

$$Org_{aq} + xH_2O \Leftrightarrow Org_{ads} + xH_2O_{aq} \quad (5)$$

where x is the size ratio, in terms of the number of water molecules replaced by an adsorbate molecule. When the equilibrium is reached, it is possible to obtain different expressions of the adsorption isotherm plots. On applying Flory–Huggins adsorption isotherm thermodynamic model [33], it was found that the experimental results at 30 °C fit well in 2 M H_3PO_4 + 0.5 M Cl^- containing different concentrations of IPMP (correlation coefficient 0.99) (see Fig. 10). The adsorption isotherm relationships of Flory–Huggins were represented by the equation:

$$\log\ \theta/C = \log xK + x\log(1-\theta) \quad (6)$$

where θ is the degree of coverage, x is the number of active sites occupied by one inhibitor molecule or number of water molecules replaced by one molecule of the adsorbate water molecules replaced by one molecule of adsorbate. Values of x greater than one imply the formation of multilayer of inhibitor on the metal surface. However, values of x less than one mean that a given inhibitor molecule would occupy more than one active site. K is the binding constant of the adsorption reaction and C is the inhibitor concentration in the bulk solution. K can be related to the standard free energy of adsorption ΔG°_{ads} by the following equation:

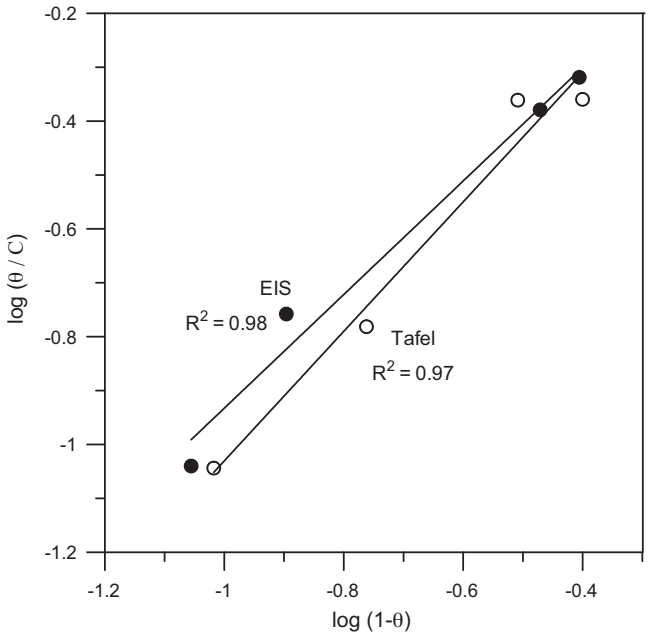

Fig. 10. Curve fitting of EIS and Tafel data of steel in 2 M H_3PO_4 + 0.5 M Cl^- containing different concentrations of IPMP to Flory–Huggins isotherm at 303 K.

$$K = \frac{1}{55.5}\exp\frac{-\Delta G^\circ_{ads}}{RT} \quad (7)$$

where R is the universal gas constant and T is the absolute temperature. The calculated values are $x = 1.05$; $K = 1258.6$ and $\Delta G^\circ_{ads} = -27.63$ kJ mol^{-1}. The number of active site, x, is close to 1. This means that, on adsorption, the inhibitor molecule displaced one water molecule. The large negative value of the standard free energy of adsorption ΔG°_{ads} denotes that the adsorption reaction proceeded spontaneously and suggests that the inhibitor adsorption was principally by chemisorption.

Since steel surface contained positive charges in the acid solution [34], results could be explained on the assumption that in the presence of Cl^-, the negatively charged Cl^- would attach to positively charged surface. Then, near the interface, the concentrations of Cl^- and protonated IPMP were much higher than those in bulk solution; the protonated IPMP did not attach directly to the positively charged steel surface because of repulsive interaction between the protonated IPMP and the positively charged steel surface. The protonated IPMP, however, could attach to the steel surface by means of electrostatic interaction between Cl^- and protonated IPMP.

3.4. Effect of temperature

It is found that the corrosion rate of the steel increases as the temperature increases. The results indicate that increasing temperature leads to a decrease of R_T, hence increasing the corrosion rate of the steel as shown in Fig. 11. A plot of $\ln i_{corr}$ vs. T^{-1} obeys Arrhenius equation [35]:

$$\ln\ i_{corr} = -\frac{E_a}{RT} + \text{const.} \quad (8)$$

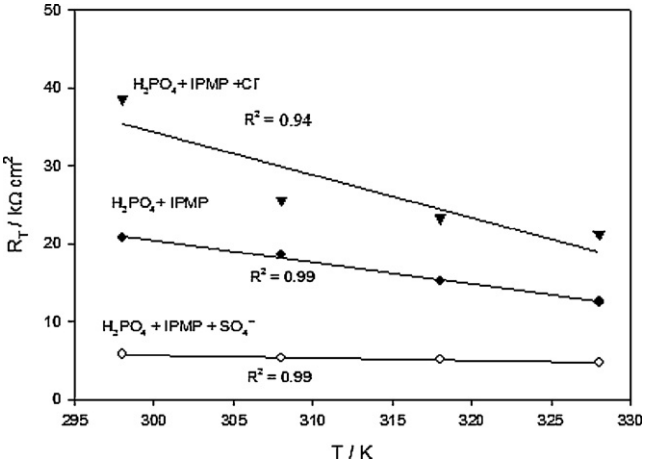

Fig. 11. Variation of R_T values of steel in 2 M H_3PO_4 + 10 mM IPMP without/with 0.5 M Cl^- or 0.5 M SO_4^{2-} at different temperatures.

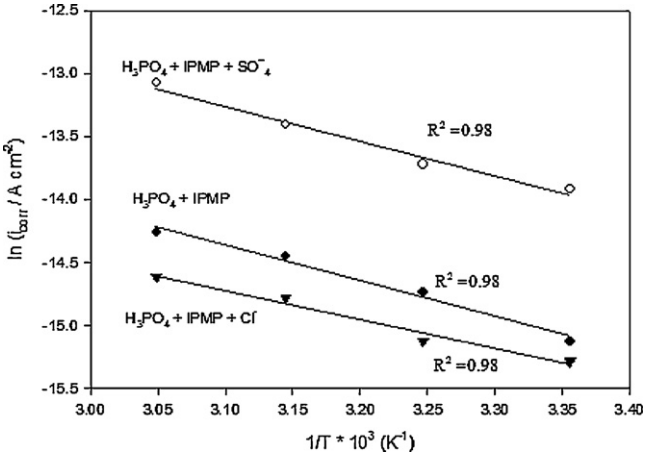

Fig. 12. Variation of $\ln i_{corr}$ with T^{-1} for steel in 2 M H_3PO_4 + 10 mM IPMP without/with 0.5 M Cl^- or 0.5 M SO_4^{2-} at different temperatures.

The relation is illustrated in Fig. 12; a straight line of Arrhenius plot was obtained. The calculated activation energy is equal to 19.1, 23.5 and 23.1 kJ mol^{-1} for 2 M H_3PO_4 + 10 mM IPMP without/with 0.5 M Cl^- or 0.5 M SO_4^{2-} respectively.

4. Conclusions

Based on the results of potentiodynamic polarization and EIS measurements at different temperatures, the following conclusions are drawn in this study:

- The values of i_{corr} increase with increasing the molar concentration of the prevailing anion (SO_4^{2-} or Cl^-) in 2 M H_3PO_4.
- At a fixed anion level from both sulphate or chloride solutions, the value of i_{corr} are higher in the H_3PO_4 solutions containing chloride electrolyte compared with the H_3PO_4 containing sulphate. This is possibly be due to the difference in the extent of incorporation by the electrolyte species during the anodization process.
- Quantitative analysis based on the CPE concept gives a better agreement between the experimental results and the theoretical data indicating the validity of the proposed model (two time constants) in explaining the experimental data.
- The order of IE (calculated from polarization and EIS data) increases as follows: H_3PO_4 + IPMP + Cl^- > H_3PO_4 + IPMP > H_3PO_4 + IPMP + SO_4^{-}.
- The total resistance R_T values increase with increasing IPMP concentration in Cl^- than in SO_4^{2-}. It is possible to assume that Cl^- can concomitantly hydrolysis reaction which generates insoluble salts or hydroxides that hinder contact between the metallic surface and the electrolyte solution with a consequent decrease in the corrosion rate associated with R_T value increase.
- At different temperatures, the results indicate that increasing temperature leads to a decrease of the total resistance value, R_T, hence increasing the corrosion rate of the mild steel even in presence of Cl^- ions.
- SEM suggesting that addition of chloride ions to IPMP inhibitor in the H_3PO_4 improves the inhibition process while addition of sulphate retards the inhibition process and this confirms the impedance and polarization results.

References

[1] P.B. Raja, M.G. Sethuraman, Materials Letters 62 (2008) 113–116.
[2] A.M. Fekry, R.R. Mohamed, Electrochimica Acta 55 (2010) 1933–1939.
[3] A.M. Fekry, M.A. Ameer, International Journal of Hydrogen Energy 35 (2010) 7641–7651.
[4] H. Amar, J. Benzakour, A. Derja, D. Villemin, B. Moreau, Journal of Electroanalytical Chemistry 558 (2003) 131–139.
[5] C. Jeyaprabha, S. Sathiyanarayanan, K.L.N. Phani, G. Venkatachari, Journal of Electroanalytical Chemistry 585 (2005) 250–255.
[6] M.A. Migahed, H.M. Mohamed, A.M. Al-Sabagh, Materials Chemistry and Physics 80 (2003) 169–175.
[7] M.A. Ameer, Materials Chemistry and Physics 122 (2010) 321–324.
[8] G. Gunasekaran, L.R. Chauhan, Electrochimica Acta 49 (2004) 4387–4395.
[9] L. Wang, Corrosion Science 43 (2001) 2281–2289.
[10] E.A. Noor, Corrosion Science 47 (2005) 33–55.
[11] A. Bellaouchou, B. Kabkab, A. Guenbour, A. Ben Bachir, Progress in Organic Coatings 41 (2001) 121–127.
[12] L.D. Muñoz, A. Bergel, D. Féron, R. Basséguy, International Journal of Hydrogen Energy 35 (2010) 8561–8568.
[13] M.A. Ameer, A.M. Fekry, International Journal of Hydrogen Energy 35 (2010) 11387–11396.
[14] M.A. Ameer, E. Khamis E, G. Al-Senani, Journal of Applied Electrochemistry 32 (2002) 149–156.
[15] E. Khamis, M.A. Ameer, N. AlAndisN., G. Al-Senani, Corrosion 56 (2000) 127–138.
[16] E. Khamis, E. El-Ashry, A. Ibrahim, British Corrosion Journal 35 (2000) 150–154.
[17] S. Ogura, K. Sugimoto, Y. Sawada, Corrosion Science 16 (1971) 323–330.
[18] A.M. Fekry, Electrochimica Acta 54 (2009) 3480–3489.
[19] A.M. Fekry, International Journal of Hydrogen Energy 35 (2010) 12945–12951.
[20] E. Khamis, N. AlAndis, Materials wiss. U. Werkstofftech. 33 (2002) 550–554.
[21] A.M. Badiea, K.N. Mohana, Journal of Materials Engineering and Performance 18 (2009) 1264–1271.
[22] X. Li, L. Tang, L. Li, G. Mu, G. Liu, Corrosion Science 48 (2006) 308–321.
[23] A. Abd El-Maksoud, Applied Surface Science 206 (2003) 129–136.
[24] E. Patrito, V. Macagno, Journal of Electroanalytical Chemistry 375 (1994) 203–211.
[25] M.A. Ameer, A.M. Fekry, A.A. Ghoniem, Corrosion 65 (2009) 587–594.
[26] M. Hepel, M. Tomkiewicz, Journal of the Electrochemical Society 132 (1985) 32–38.
[27] P. Bruzzoni, R.M. Carranza, International Journal of Hydrogen Energy 25 (2000) 61–65.
[28] M.A. Ameer, A.M. Fekry, F.E. Heakal, Electrochimica Acta 50 (2004) 43–49.
[29] G. Mu, X. Li, F. Li, Materials Chemistry and Physics 86 (2004) 59–68.
[30] P.C. Okafor, M.E. Ikpi, I.E. UwahaE, E.E. Ebenso, U.J. Ekpe, S.A. Umoren, Corrosion Science 50 (2008) 2310–2317.
[31] P.C. Okafor, E.E. Ebenso, U.J. Ekpe, International Journal of Electrochemical Science 5 (2010) 978–993.
[32] J.A. Jaen, E. Garcia de Saldana, C. Hernandez, Hyperf. International 122 (1999) 139–145.
[33] H. Takata, N. Mizuno, M. Nishikawa, S. Fukada, M. Yoshitake, International Journal of Hydrogen Energy 32 (2007) 371–379.
[34] A. Ostovari, S.M. Hoseinieh, M. Peikari, S.R. Shadizadeh, S.J. Hashemi, Corrosion Science 51 (2009) 1935–1949.
[35] P.W. Atkin, Physical Chemistry, 5th ed., University Press, Oxford, 1994, p. 877.